Optimized Operation of Quantum-Dot Intermediate-Band Solar Cells Deduced from Electronic Transport Modeling

Nicolas Cavassilas,[1,*] Daniel Suchet,[2] Amaury Delamarre,[3] Jean-Francois Guillemoles,[4] Fabienne Michelini,[1] Marc Bescond,[5] and Michel Lannoo[1]

[1] *Aix Marseille Université, CNRS, Université de Toulon, IM2NP UMR 7334, 13397 Marseille, France*
[2] *Ecole Polytechnique, Institut Photovoltaïque d'Ile-de-France, 30 RD 128, 91120 Palaiseau, France*
[3] *Centre de Nanosciences et de Nanotechnologies, 91120 Palaiseau, France*
[4] *Institut Photovoltaïque d'Ile-de-France, 30 RD 128, 91120 Palaiseau, France*
[5] *LIMMS, CNRS Institute of Industrial Science, UMI 2820, University of Tokyo, Tokyo, 153-8505, Japan*

(Received 15 October 2019; revised manuscript received 10 December 2019; accepted 23 March 2020; published 13 April 2020)

Study of the physics of quantum electronic transport has not tackled the problems raised by quantum-dot intermediate-band solar cells. Our study shows that this physics imposes design rules for the intersubband transition. We develop an analytical model that correctly treats, from a quantum point of view, the trade-off between the absorption, the recombination, and the electronic transport occurring in this transition. Our results clearly indicate that it is essential to control the transit rate between the excited state of the quantum dot and the embedding semiconductor. For that, we propose assuming the dot in a tunnel shell whose main characteristics can be obtained by a simple analytical formula. Moreover, we show that in a realistic case, the energy transition needs to be larger than only 0.27 eV to obtain a quasi-Fermi-level-splitting. This quite small value designates the quantum-dot solar cell as a serious candidate to be an efficient intermediate-band solar cell. This work gives a framework to design efficient intersubband transitions and opens new opportunities for quantum-dot intermediate-band solar cells.

DOI: 10.1103/PhysRevApplied.13.044035

I. INTRODUCTION

Intersubband transitions are widely used in infrared sensors [1] and in the concept of intermediate-band solar cells (IBSCs) [2]. From an optical point of view these transitions have been the subject of numerous studies that show that the monochromatic absorption is maximum between the ground state and the first excited state if they are well localized (bound-to-bound system) [3]. Nevertheless, whether in sensors or in solar cells, the objective is to recover excited electrons in an electric current. In the case of sensors this current is the response to the absorption, while in a solar cell it is the origin of the generated power. However, in the case where the electrons were excited in a very localized state, it will be difficult to extract them in an electrical contact. On the other hand, the reduction of the localization decreases the maximum absorption but also broadens the absorption. This could be an advantage for a wide-spectrum excitation. Finally, we understand that it will be necessary to find a compromise between absorption, recombination, and extraction [4].

In this paper we propose an analytical model in which all these effects are considered rigorously from the point of view of quantum mechanics. We have developed this model on the basis of the nonequilibrium-Green-functions (NEGF) formalism that allows us to treat a quantum system with interactions [5–9]. The system, in this case a quantum dot with a tunnel shell embedded in a three-dimensional material, is simplified for computational reasons. The main simplifications are a perfectly selective contact, flat bands, and the effective-mass approximation. This gives an effective model that, with a reduced number of parameters, favors the understanding of difficult but ultimately very-important quantum-transport phenomena. Moreover, even if such approaches are not as precise as fully numerical models, effective models are currently used to optimize devices assuming, for example, a strongly confined system [10,11], tunneling modified by strain [12], or scattering in a quantum well [13].

This analytical model is then applied to the intersubband transition of an IBSC. The purpose of this concept is to exceed the Shockley-Queisser limit [14] by using an intermediate band in the band gap of the absorbing semiconductor [15,16]. The idea is to use this intermediate band to absorb photons having a lower energy than the band gap. This absorption is then supposed to contribute to the current [17] without the full loss in voltage of a simple band-gap solar cell. To create an intermediate band,

*nicolas.cavassilas@im2np.fr

 © 2020 American Physical Society

nano-objects (usually dots) are often used [2,18,19]. Their lowest conduction state serves as an intermediate band, while the second lowest is connected to the contact. But this concept has not yet demonstrated performance beyond the Shockley-Queisser limit [19]. The main difficulty is that electronic populations in the intermediate band and in the contact must not be allowed to equilibrate, so as to maintain a quasi-Fermi-level-splitting. Without this splitting, the IBSC is reduced to a simple solar cell with the band gap defined by the energy between the valence-band and the first conduction state of the nano-objects. This is usually obtained experimentally. In this article, we investigate in depth this intersubband transition between the first two conduction states of the dot.

We have already reported a study dedicated to this transition [4], but the conclusions were limited to a specific case (one set of parameters). With the present analytical model, it is possible to extend this study and to draw more-general conclusions. We show that this transition must follow some rules, related to quantum electronic transport, in order to provide efficiency higher than that of an equivalent single-band-gap solar cell. To the best of our knowledge, none of these rules have ever been respected in a quantum-dot IBSC proposed in the literature. Our findings, therefore, offer new perspectives by providing a framework for the design of an IBSC.

II. MODEL AND SYSTEM

The system we model is schematically represented in Fig. 1. It is characterized by a discrete state $|1\rangle$ of energy E_1 filled with an energy-independent distribution f_1 that is considered as an input parameter. This state represents the intermediate band and f_1 the filling of this band. In an IBSC, f_1 is also relative to the transition between the valence band and the intermediate band. Even though this transition is another technological challenge involving the transport of holes, here we consider it only through this filling parameter. In addition to the first state $|1\rangle$, which is perfectly located in the quantum dot, we consider an excited state $|2\rangle$ at E_2 (the transition energy is given by $E_t = E_2 - E_1$) that has a coupling strength to the contact tuned via a tunnel barrier. The characteristics of this barrier result in a tunnel transfer rate σ_T. Tunneling can occur in both ways, either by extraction of generated carriers from $|2\rangle$ to the contact or by injection of carriers from the contact into $|2\rangle$ for a retrapping. As far as emission and absorption are concerned, states $|1\rangle$ and $|2\rangle$ are both linked by σ_I and σ_S, the induced and spontaneous optical transition rates, respectively. Moreover, as stated in Sec. I, states $|1\rangle$ and $|2\rangle$ and the contact do not share the same distribution. We then consider a second Fermi function for the contact f_c. In an illuminated IBSC, the two corresponding chemical potentials μ_c and μ_1 must be split so that there is a gain compared with a single-band-gap solar cell.

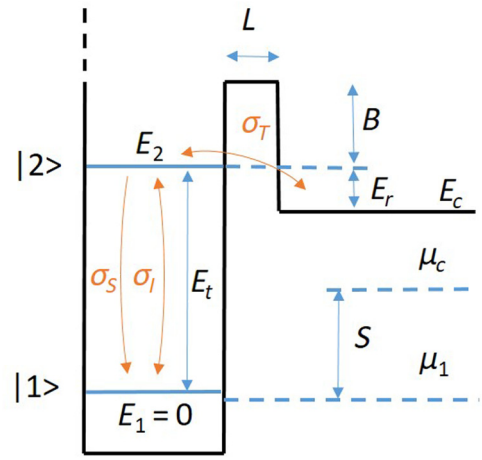

FIG. 1. Band diagram of the dot with the tunnel shell embedded in a three-dimenional material. We assume flat bands and a perfect selected contact (infinite barrier on the left). The input parameters are the energy E_1 of the ground state $|1\rangle$ (the intermediate band), the energy E_2 of the excited state $|2\rangle$, the height B and the thickness L of the barrier, and the energy of the band edge of the contact E_c. Concerning transport, states $|1\rangle$ and $|2\rangle$ and the contact are coupled by tunneling (σ_T) and induced and spontaneous optical couplings (σ_I and σ_S). In all the present study, the origin of energy is $E_1 = 0$.

In our model this quasi-Fermi-level-splitting, $S = \mu_c - \mu_1$, is an input parameter. Finally, the contact is also defined by its band-edge energy E_c, and in the following we call $E_r = E_2 - E_c$ the ratchet energy [20–25].

To calculate the current generated by this transition, we use detailed-balance model with radiative and tunneling rates calculated with the NEGF formalism. It is very powerful since it allows us to consider a quantum system with interactions. The interaction between photons and electrons is processed by a self-energy that represents the central concept to describe inelastic scattering in the Green's functions. In the literature this is usually done numerically [5,7,26]. Here, by simplifying the description of the system (through the flat-band approximation in particular), we can include it analytically. For example it allows us to calculate the tunnel transit rate from state $|2\rangle$ through the tunnel barrier [27]:

$$\sigma_T = \frac{8E_2}{3\hbar k_r W \cosh^2 L\rho}, \tag{1}$$

where $W = \hbar\pi/\sqrt{2E_t m^*/3}$ is the side length of the cubic dot and L is the thickness of the tunnel barrier. The wave vectors of the electron at energy E in the contact (with origin $E_1 = 0$) and the barrier are respectively given by $k_r = \sqrt{2(E_2 - E_c)m^*}/\hbar$, where m^* is the effective mass, and $\rho = \sqrt{2Bm^*}/\hbar$, where B is the barrier energy related to E_2. As expected this expression shows that the tunnel transit rate σ_T decreases exponentially with L. Moreover,

it shows that when E_2 is close to E_c (low k_r), an interference behavior increases the tunnel rate. Note finally that this expression is original. It is related to the tunneling between a continuum and a quasicontinuum [28], and is not related to the tunneling between two continua or to a resonant tunneling on a bound state [29,30].

See Supplemental Material [27] for the analytical development of the tunnel transit expression, like the development of the current formula resulting in Eq. (4). Before we provide this full expression, we present another formula, with a similar form, but obtained with a simpler development based on the rate model. This toy model helps us better understand the final formula.

For this toy model, we assume discrete states for $|1\rangle$ and $|2\rangle$ and the contact. Moreover, σ_T and both optical rates σ_I and σ_S are independent of the energy. It is then straightforward to write the variation in time of the distribution f_2 on state $|2\rangle$ knowing f_1 and f_c:

$$\frac{df_2}{dt} = \sigma_T[f_c(1-f_2) - f_2(1-f_c)] + \sigma_I[f_1(1-f_2) - f_2(1-f_1)] - \sigma_S f_2(1-f_1). \quad (2)$$

In the steady state this variation vanishes. Assuming this condition, and knowing that the current at the contact is given by $J = -e\sigma_T(f_2 - f_c)$ (e is the elementary charge), we then have for the current

$$J = e\sigma_T \frac{\sigma_I(f_c - f_1) + \sigma_S f_c(1-f_1)}{\sigma_T + \sigma_I + \sigma_S(1-f_1)}. \quad (3)$$

This expression shows that the current is a competition between induced absorption and spontaneous recombination (in the numerator). This competition is all-the-more favorable for absorption as f_1 is high and f_c is low. The technological challenge is to have higher generation than recombination while having a higher chemical potential in the contact than in state $|1\rangle$. Concerning the trade-off between tunneling and optical processes, the numerator is given by the product of σ_T and the summation of the optical rates, while the denominator equals the summation of all rates. Therefore, if σ_T is much larger than the optical rates, the current is limited by the optical processes. In the opposite situation, the current is limited by the tunneling. This then confirms that the current is a balance between all such interactions.

The main limit of this toy model is that the density of states of $|2\rangle$ is a simple Dirac peak. Because this state is linked to both state $|1\rangle$ and the contact, the lifetime is finite. This implies, according to the uncertainty relation, that state $|2\rangle$ is broadened [5,31]. We see in the following that this broadening is the key element to obtain maximum efficiency. As shown in Supplemental Material [27], by considering the calculation of the transit rates via the NEGF formalism, we go beyond the previous toy model [Eq. (3)] and obtain for the current across the system presented in Fig. 1 the following expression:

$$\begin{aligned} J(S) &= \int_{E_c}^{E_m} J(S,E)dE \\ &= \int_{E_c}^{E_m} [J_A(S,E) + J_R(S,E)]dE = \frac{2e}{h}\int_{E_c}^{E_m} \sigma_T \\ &\quad \times \frac{\sigma_I(E)[f_c(E) - f_1] + \sigma_S(E) f_c(E)(1-f_1)}{(\frac{E-E_2}{\hbar})^2 + [\sigma_T + \sigma_I(E) + \sigma_S(E)(1-f_1)]^2} dE. \end{aligned} \quad (4)$$

The absorption current $J_A(S,E)$ is related to the induced optical rate $\sigma_I(E) = [\mathcal{M}(E)/\hbar][C\Omega_S b_{T_S}(E) + n_r \pi b_{T_R}(E)]$, while the retrapping current $J_R(S,E)$ is related to the spontaneous optical rate $\sigma_S(E) = [\mathcal{M}(E)/\hbar] n_r \pi$, where $b_T(E) = 1/[\exp(E/k_B T) - 1]$ is the Bose distribution, $T_S = 6000$ K and $T_R = 300$ K are the Sun temperature and room temperature, respectively, and $\Omega_S = 6.7 \times 10^{-5}$ is the solid angle of absorption. The electron-photon coupling, assuming plane waves in the pseudopotential approach [31,32], is given by

$$\mathcal{M}(E) = \frac{\hbar n}{2\pi^2 \epsilon_0 c^3}\left(\frac{8e}{3m^* W}\right)^2 E, \quad (5)$$

where n is the refractive index of the material considered. We also have $f_c(E) = 1/\{1 + \exp[(E - \mu_c)/k_B T_R]\}$. Concerning the sign convention for the current, power is produced when $J < 0$. For all calculations, we choose a half-filled initial state, with $f_1 = 0.5$, involving $\mu_1 = E_1$. See Supplemental Material [27] for the definition of the upper limit E_m. Finally, C is the Sun concentration and n_r is a nonradiative coefficient that accounts for nonradiative recombination: for one radiative recombination we have $(n_r - 1)$ nonradiative recombinations [33]. This parameter strongly depends on the materials, growing conditions, and shape of the dots [34]. In consequence, while experimental study shows results close to the radiative limit [34,35], theoretical calculations suggest $n_r = 5 \times 10^4$ [36]. In the following, we generally assume $n_r = 100$ but we extended our conclusions to the radiative limit and to the case where strong nonradiative processes occur.

The denominator of Eq. (4) looks like that of a Lorentzian centered at E_2, while the numerator looks like that of Eq. (3). Indeed, in both Eq. (3) and Eq. (4), the current is proportional to the tunnel transit rate σ_T and is a competition between absorption and retrapping. But compared with Eq. (3), the denominator of Eq. (4) shows a broadening around E_2 that is given by the sum of the different transition rates. A fast analysis of this equation shows that $J(0, E_2)$ is maximum when $\sigma_T = \sigma_I(E_2) + \sigma_S(E_2)(1 - f_1)$. If σ_T is lower, the current is limited by tunneling, while if it is larger, the current is limited by

absorption. This condition does not involve that the current being maximum since the total current is the result of a summation over energy. However, as we show later, adjusting the design to fulfill this condition remains a good milestone.

As shown in Supplemental Material [27], we can note finally that this set of equations can easily be implemented in a few lines of code. Using Eq. (4), we can calculate the current spectrum and the total current as a function of S for the junction shown in Fig. 1. If we consider this intersubband transition as a solar cell, we can calculate the corresponding short-circuit current $J_{SC} = J(S = 0)$, the open-circuit quasi-Fermi-level-splitting S_{OC} canceling the current, and the maximum power P_{max}.

III. RESULTS

Figure 2 shows current spectra at S_{OC} for a realistic set of parameters and different tunnel-barrier thicknesses. The negative (positive) component corresponds to absorption (retrapping). The narrower around E_2 these two components are, the thicker is the barrier. This reflects the effect of the lifetime on the broadening of $|2\rangle$ controlled by the tunneling rate. For recombination, in addition to this peak, there are also electrons injected from the contact band edge at E_c. This contribution is all-the-more important as the broadening of $|2\rangle$ is important. Indeed, a high density of states in the well at energy E_c promotes the injection from the contact. In the bound-to-continuum case ($L = 0$ nm) shown in Fig. 2(a), the broadening is maximum and this band-edge injection is dominant. As a result, S_{OC} is low since it is controlled by E_c and not by E_2. This band edge also impacts the current absorption since, as shown Fig. 2(a), the spectrum is cut off at E_c. Therefore, in the case of large broadening of $|2\rangle$, the effective energy transition is more defined by E_c than by E_2 in the sense that low (high) E_c means high (low) J_{SC} and low (high) S_{OC}.

Figure 2(b) shows the current spectrum in the bound-to-bound case with a thick barrier, $L = 12$ nm. The broadening being small, we have a very weak injection from E_c and consequently a higher S_{OC} than in the bound-to-continuum case. We recover here the *broadening effect* introduced in previous work [4] at the origin of S_{OC} modification. Moreover, because the excitation component is very narrow around E_2, the absorption spectrum is no longer cut off at E_c. In this case, the effective energy of the intersubband transition is defined by E_2. However, despite a higher S_{OC}, the power is just a little greater than in the bound-to-continuum case. The current is indeed limited since the excited electrons hardly tunnel through the contact. The best trade-off between absorption, extraction, and recombination is obtained for the intermediate case shown in Fig. 2(c), where $L = 6$ nm. The consequence of the corresponding moderate broadening is a much larger current and an intermediate S_{OC}. Compared with the usually assumed bound-to-bound case, the current and the power are increased by a ratio of 3 and 5, respectively.

These results show that it is essential to control the broadening of state $|2\rangle$ via σ_T to have a good balance between all transport processes. For that, as we already suggested in Ref. [4], a well-designed tunnel barrier is a relevant solution. While the bound-to-continuum case is generally considered in IBSCs [37–40], some studies assume the quantum dot is embedded in a large-band-gap material [41–45]. This last solution is proposed to reduce the strain and the corresponding structural defects, but it could also make it possible to control the tunnel transit and hence the broadening of the excited state. It is also possible to design a dot directly in the host material, without a shell, if both the band offset and the dot size are sufficient to have a localized excited state. In this case, the tunnel barrier between the dot and the contact has to be controlled by an electric field generated by doping and/or built-in charge [46].

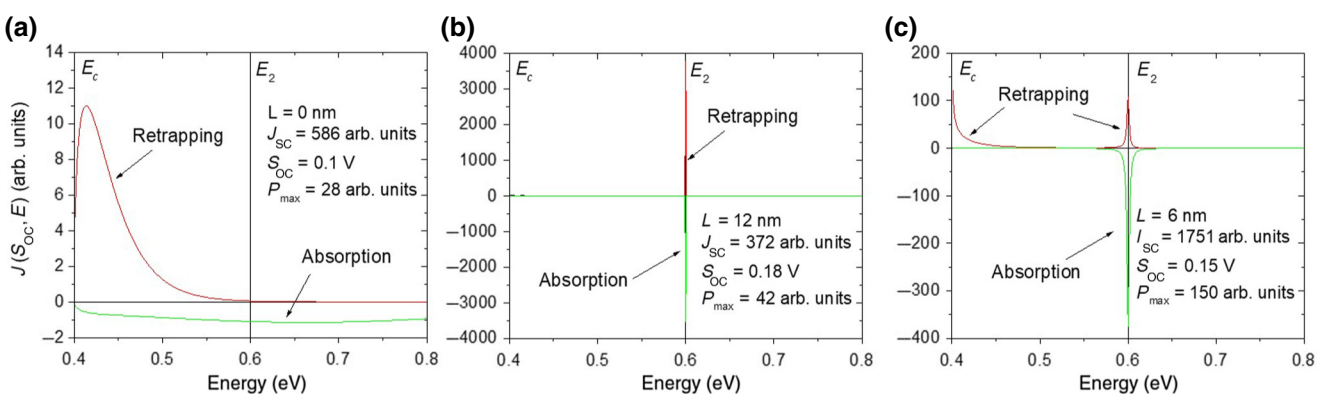

FIG. 2. Current spectrum, calculated at S_{OC} for $B = 0.2$ eV, $m^* = 0.07m_0$ (m_0 is the free-electron mass), $n = 3.5$, $n_r = 100$, $E_t = 0.6$ eV, $E_r = 0.2$ eV, $E_m = 1.4$ eV, and (a) $L = 0$ nm, (b) $L = 10$ nm, or (c) $L = 5$ nm. The absorption current $J_A(S_{OC}, E)$ is represented by the green line and the retrapping current $J_R(S_{OC}, E)$ is represented by the red line. For each value of L we also show J_{SC}, S_{OC}, and P_{max}.

The optimal barrier thickness depends on all parameters and the precedent value of 5 nm cannot be generalized. To offer an extended study, it would be interesting to have an expression estimating such an optimal barrier thickness. For that, we remember that the current $J(0, E_2)$ is maximum when $\sigma_T(E_2) = \sigma_I(E_2) + \sigma_S(E_2)(1 - f_1)$, and checking that $\sigma_I \ll \sigma_S$, we propose an expression allowing us to estimate the best trade-off: $\sigma_T(E_2) = \alpha(n_r)\sigma_S(E_c)$, where $\alpha(n_r) = 60\exp[\log_{10} n_r - 1]$. Considering this condition in Eq. (4), we extract an expression that estimates the optimal thickness of the tunnel barrier, L_{opt}, according to all the other parameters:

$$L_{\text{opt}} = \frac{1}{\rho}\ln\left(\frac{\sqrt{\frac{8E_t}{3k_rW}} + \sqrt{\frac{8E_t}{3k_rW} - M(E_c)\pi n_r\alpha(n_r)(1 - f_1)}}{\sqrt{M(E_c)\pi n_r\alpha(n_r)(1 - f_1)}}\right). \tag{6}$$

This expression shows that, for example, in the case of a large nonradiative coefficient n_r and/or low f_1, the retrapping is naturally large and L should be chosen small to preserve a large σ_T. In contrast, close to the radiative limit, L should be large. We note also that all parameters modifying σ_T also play a role, which includes k_r related to the ratchet energy and E_t and W both related to the dot design. Figure 3 illustrates the impact of the recombination by representing the maximum power versus L [calculated with Eq. (4)] for various values of n_r. These curves, in addition to illustrating the advantage of considering a tunnel barrier, confirm the good estimation of L_{opt} given by Eq. (6).

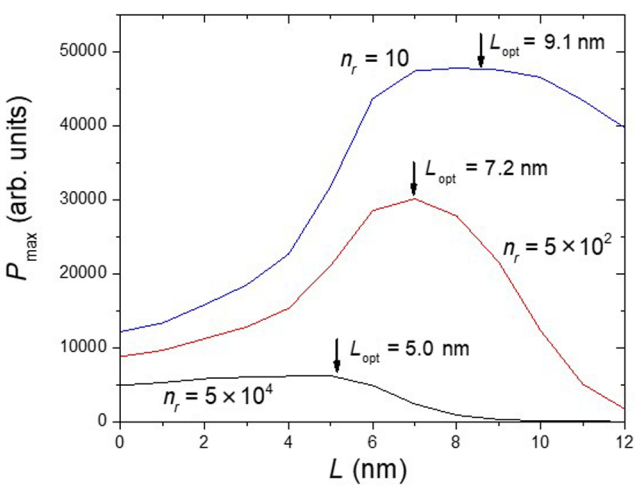

FIG. 3. Maximum power $P_{\max}$ versus tunnel-barrier thickness L extracted from the J-V characteristic calculated with Eq. (4) for $B = 0.2$ eV, $m^* = 0.07m_0$ (m_0 is the free-electron mass), $n = 3.5$, $E_t = 0.6$ eV, $E_r = 20$ meV, $C = 500$, and various values of n_r. We also report the estimation of the optimal thickness L_{opt} obtained with Eq. (6). To estimate the precision of this equation, these values can be compared with the top position of the corresponding curves.

TABLE I. The minima of energy for the intermediate-band-to-conduction-band transition calculated for several concentrations C and nonradiative coefficients n_r. E_{quant}, calculated with our model, corresponds to the limit under which the intersubband transition cannot produce power. E_{classic}, calculated with a detailed-balance model assuming sharp absorption, corresponds to the limit under which the IBSC is less efficient that the optimal single-band-gap solar cell.

C	n_r	1	100	5×10^4
1	E_{quant}	0.15	0.27	0.43
	E_{classic}	0.14	0.30	0.49
500	E_{quant}		0.11	0.27
	E_{classic}		0.08	0.30
10^4	E_{quant}		0.03	0.19
	E_{classic}		0.02	0.20

Finally, we can estimate with use of our model the minimum transition energy allowing the generation of power with the intersubband transition considered. Reducing E_t and consequently E_c involves an increase of the injection from the contact. If, at $V = 0$ V, the retrapping current is of the same order of magnitude as the absorption current, application of any quasi-Fermi-level-splitting is impossible. For example, for $n_r = 100$ and $C = 1$, we find that E_t has to be larger than 0.27 eV. We calculate this limit, called E_{quant}, for several concentrations and nonradiative factors as shown in Table I.

Regardless of the present study, the optical transitions in IBSCs must be large enough for such cells to offer higher efficiency than the optimal single-band-gap solar cell. As shown in Supplemental Material [27], this limit can be estimated with a classical detailed-balance model considering the three optical transitions of the IBSC [24]. In Table I, we compare this classical limit E_{classic} with the quantum limit E_{quant}. These two limits are, in any case, very close. This means that the intersubband character of the transition, if it is well designed, does not increase the limitation to obtain an efficient IBSC. This validates the use of quantum dots as a judicious choice for the IBSC.

IV. CONCLUSION

In conclusion, we present a theoretical study on the intersubband transition in quantum-dot IBSCs. For this, we develop a rigorous model, but one that is nevertheless easy to implement. Using this model, we give recommendations for designing an efficient intersubband transition. Considering a realistic recombination rate, the transition energy E_t between the intermediate band and the excited state must be greater than 0.27 eV without concentration and 0.11 eV under 500 suns. Under this limit, the intermediate band is in thermodynamic equilibrium with the contact. Above this limit, the tunneling rate has to be controlled by a tunnel barrier. In the radiative limit, this barrier should be thick,

while it should be thinner when the nonradiative processes increase. In the case where the optimal design suggests a thick barrier, an energy ratchet may be considered without any damage because tunneling from E_c to the dot is reduced. Such a ratchet could represent an advantage, since as we saw in another study [22,23], the degrees of freedom on E_r make it possible to match the different transitions of the IBSC. On the other hand, in case of a thin barrier, both S_{OC} and J_{SC} are controlled by such a ratchet energy. This parameter has then to be carefully chosen using Eq. (4).

This study confirms that obtaining an efficient IBSC involves significant technological challenges, particularly for the band offsets in order to achieve a sufficiently large E_t. On the other hand, we show that the intersubband character of the transition does not worsen these conditions and we confirm that quasi-Fermi-level-splitting can be achieved, even if the nonradiative processes are huge.

Finally, it is important to note that the analytical model presented in this work is not only dedicated to the IBSC. It may also be useful for other devices with an intersubband transition such as a photodetector or a laser.

ACKNOWLEDGMENT

The authors thank ICEMAN (Grant No. ANR-19-CE05-000) for financial support.

[1] Pierre-Baptiste Vigneron, Stefano Pirotta, Iacopo Carusotto, Ngoc-Linh Tran, Giorgio Biasiol, Jean-Michel Manceau, Adel Bousseksou, and Raffaele Colombelli, Quantum well infrared photo-detectors operating in the strong light-matter coupling regime, Appl. Phys. Lett. **114**, 131104 (2019).

[2] Stanko Tomić, Tomah Sogabe, and Yoshitaka Okada, In-plane coupling effect on absorption coefficients of InAs/GaAs quantum dots arrays for intermediate band solar cell: In-plane coupling effect on absorption coefficients of InAs/GaAs quantum dots arrays, Prog. Photovolt.: Res. Appl. **23**, 546 (2015).

[3] B. F. Levine, A. Zussman, S. D. Gunapala, M. T. Asom, J. M. Kuo, and W. S. Hobson, Photoexcited escape probability, optical gain, and noise in quantum well infrared photodetectors, J. Appl. Phys. **72**, 4429 (1992).

[4] Nicolas Cavassilas, Daniel Suchet, Amaury Delamarre, Fabienne Michelini, Marc Bescond, Yoshitaka Okada, Masakazu Sugiyama, and Jean-Francois Guillemoles, Beneficial impact of a thin tunnel barrier in quantum well intermediate-band solar cell, EPJ Photovolt. **9**, 11 (2018).

[5] Nicolas Cavassilas, Fabienne Michelini, and Marc Bescond, Modeling of nanoscale solar cells: The Green's function formalism, J. Renew. Sustain. Energy **6**, 011203 (2013).

[6] Nicolas Cavassilas, Fabienne Michelini, and Marc Bescond, On the local approximation of the electron-photon interaction self-energy, J. Comput. Electron. **15**, 1233 (2016).

[7] Urs Aeberhard and Uwe Rau, Microscopic Perspective on Photovoltaic Reciprocity in Ultrathin Solar Cells, Phys. Rev. Lett. **118**, 247702 (2017).

[8] Aude Berbezier and Urs Aeberhard, Impact of Nanostructure Configuration on the Photovoltaic Performance of Quantum-Dot Arrays, Phys. Rev. Appl. **4**, 0 (2015).

[9] M. Luisier, A. Szabo, C. Stieger, C. Klinkert, S. Bruck, A. Jain, and L. Novotny, *First-Principles Simulations of 2-D Semiconductor Devices: Mobility, I–V Characteristics, and Contact Resistance* (IEEE, San Francisco, 2016), pp. 5.4.1–5.4.4.

[10] K. Nehari, M. Lannoo, F. Michelini, N. Cavassilas, M. Bescond, and J. L. Autran, Improved effective mass theory for silicon nanostructures, Appl. Phys. Lett. **93**, 092103 (2008).

[11] Cristina Medina-Bailon, Toufik Sadi, Mihail Nedjalkov, Hamilton Carrillo-Nunez, Jaehyun Lee, Oves Badami, Vihar Georgiev, Siegfried Selberherr, and Asen Asenov, Mobility of circular and elliptical Si Nanowire transistors using a multi-subband 1D formalism, IEEE Electron Device Lett. **40**, 1571 (2019).

[12] Lei Liu, Renrong Liang, Jing Wang, and Jun Xu, Enhanced carrier mobility and direct tunneling probability of biaxially strained $Ge_{1-x}Sn_x$ alloys for field-effect transistors applications, J. Appl. Phys. **117**, 184501 (2015).

[13] Aymen Yangui, Marc Bescond, Tifei Yan, Naomi Nagai, and Kazuhiko Hirakawa, Evaporative electron cooling in asymmetric double barrier semiconductor heterostructures, Nat. Commun. **10**, 0 (2019).

[14] William Shockley and Hans J. Queisser, Detailed balance limit of efficiency of p-n junction solar cells, J. Appl. Phys. **32**, 510 (1961).

[15] Antonio Luque, Antonio Martí, and Colin Stanley, Understanding intermediate-band solar cells, Nat. Photonics **6**, 146 (2012).

[16] Antonio Luque and Antonio Martí, Increasing the Efficiency of Ideal Solar Cells by Photon Induced Transitions at Intermediate Levels, Phys. Rev. Lett. **78**, 5014 (1997).

[17] Nair Lopez, Kin Man Yu, Tooru Tanaka, and Wladyslaw Walukiewicz, Multicolor electroluminescence from intermediate band solar cell structures, Adv. Energy Mater. **6**, 1501820 (2016).

[18] Tomah Sogabe, Yasushi Shoji, Mitsuyoshi Ohba, Katsuhisa Yoshida, Ryo Tamaki, Hwen-Fen Hong, Chih-Hung Wu, Cherng-Tsong Kuo, Stanko Tomić, and Yoshitaka Okada, Intermediate-band dynamics of quantum dots solar cell in concentrator photovoltaic modules, Sci. Rep. **4**, srep04792 (2014).

[19] Y. Okada, N. J. Ekins-Daukes, T. Kita, R. Tamaki, M. Yoshida, A. Pusch, O. Hess, C. C. Phillips, D. J. Farrell, K. Yoshida, N. Ahsan, Y. Shoji, T. Sogabe, and J.-F. Guillemoles, Intermediate band solar cells: Recent progress and future directions, Appl. Phys. Rev. **2**, 021302 (2015).

[20] Andreas Pusch and Nicholas J. Ekins-Daukes, Voltage Matching, Étendue, and Ratchet Steps in Advanced-Concept Solar Cells, Phys. Rev. Appl. **12**, 0 (2019).

[21] Andreas Pusch, Megumi Yoshida, Nicholas P. Hylton, Alexander Mellor, Chris C. Phillips, Ortwin Hess, and Nicholas J. Ekins-Daukes, Limiting efficiencies for intermediate band solar cells with partial absorptivity: The case

for a quantum ratchet, Prog. Photovolt.: Res. Appl. **24**, 656 (2016).

[22] Amaury Delamarre, Daniel Suchet, Masakazu Sugiyama, Nicolas Cavassilas, Yoshitaka Okada, and Jean-François Guillemoles, *Non-Ideal Nanostructured Intermediate Band Solar Cells with an Electronic Ratchet* (SPIE, San Francisco, 2018), p. 27.

[23] Daniel Suchet, Amaury Delamarre, Nicolas Cavassilas, Zacharie Jehl, Yoshitaka Okada, Masakazu Sugiyama, and Jean-Francois Guillemoles, Analytical optimization of intermediate band systems: Achieving the best of two worlds, Prog. Photovolt.: Res. Appl. **26**, 800 (2018).

[24] Amaury Delamarre, Daniel Suchet, Nicolas Cavassilas, Yoshitaka Okada, Masakazu Sugiyama, and Jean-Francois Guillemoles, An electronic ratchet is required in nanostructured intermediate-band solar cells, IEEE J. Photovolt. **8**, 1553 (2018).

[25] M. Yoshida, N. J. Ekins-Daukes, D. J. Farrell, and C. C. Phillips, Photon ratchet intermediate band solar cells, Appl. Phys. Lett. **100**, 263902 (2012).

[26] Supriyo Datta, Nanoscale device modeling: The Green's function method, Superlattices Microstruct. **28**, 253 (2000).

[27] See Supplemental Material at http://link.aps.org/supplemental/10.1103/PhysRevApplied.13.044035 for the analytical development of the tunnel-transit expression, the analytical development of the current formula resulting in Eq. (4), the estimation of the upper limit for integration in Eq. (4), and the classical detailed-balance model.

[28] R. Clerc, A. Spinelli, G. Ghibaudo, and G. Pananakakis, Theory of direct tunneling current in metal-oxide-semiconductor structures, J. Appl. Phys. **91**, 1400 (2002).

[29] Andrew Pan and Chi On Chui, Modeling direct interband tunneling. II. Lower-dimensional structures, J. Appl. Phys. **116**, 054509 (2014).

[30] Andrew Pan and Chi On Chui, Modeling direct interband tunneling. I. Bulk semiconductors, J. Appl. Phys. **116**, 054508 (2014).

[31] G. Bastard, *Wave Mechanics Applied to Semiconductor Heterostructures*, Monographies de Physique (Les Editions de Physique, 1988) .

[32] Truman O. Woodruff, in *Solid State Physics* (Elsevier, 1957), Vol. 4, pp. 367–411.

[33] M. A. Steiner, J. F. Geisz, I. García, D. J. Friedman, A. Duda, and S. R. Kurtz, Optical enhancement of the open-circuit voltage in high quality GaAs solar cells, J. Appl. Phys. **113**, 123109 (2013).

[34] Brian D. Gerardot, Daniel Brunner, Paul A. Dalgarno, Patrik Öhberg, Stefan Seidl, Martin Kroner, Khaled Karrai, Nick G. Stoltz, Pierre M. Petroff, and Richard J. Warburton, Optical pumping of a single hole spin in a quantum dot, Nature **451**, 441 (2008).

[35] Gustavo A. Narvaez, Gabriel Bester, and Alex Zunger, Carrier relaxation mechanisms in self-assembled (In,Ga)As/GaAs quantum dots: Efficient P → S Auger relaxation of electrons, Phys. Rev. B. **74**, 075403 (2006).

[36] Stanko Tomić, Intermediate-band solar cells: Influence of band formation on dynamical processes in InAs/GaAs quantum dot arrays, Phys. Rev. B **82**, 0 (2010).

[37] Denis Guimard, Ryo Morihara, Damien Bordel, Katsuaki Tanabe, Yuki Wakayama, Masao Nishioka, and Yasuhiko Arakawa, Fabrication of InAs/GaAs quantum dot solar cells with enhanced photocurrent and without degradation of open circuit voltage, Appl. Phys. Lett. **96**, 203507 (2010).

[38] F. K. Tutu, J. Wu, P. Lam, M. Tang, N. Miyashita, Y. Okada, J. Wilson, R. Allison, and H. Liu, Antimony mediated growth of high-density InAs quantum dots for photovoltaic cells, Appl. Phys. Lett. **103**, 043901 (2013).

[39] Phu Lam, Sabina Hatch, Jiang Wu, Mingchu Tang, Vitaliy G. Dorogan, Yuriy I. Mazur, Gregory J. Salamo, Iñigo Ramiro, Alwyn Seeds, and Huiyun Liu, Voltage recovery in charged InAs/GaAs quantum dot solar cells, Nano Energy **6**, 159 (2014).

[40] Neil S. Beattie, Patrick See, Guillaume Zoppi, Palat M. Ushasree, Martial Duchamp, Ian Farrer, David A. Ritchie, and Stanko Tomić, Quantum engineering of InAs/GaAs quantum dot based intermediate band solar cells, ACS Photonics **4**, 2745 (2017).

[41] Guodan Wei and Stephen R. Forrest, Intermediate-band solar cells employing quantum dots embedded in an energy fence barrier, Nano Lett. **7**, 218 (2007).

[42] S. M. Hubbard, C. D. Cress, C. G. Bailey, R. P. Raffaelle, S. G. Bailey, and D. M. Wilt, Effect of strain compensation on quantum dot enhanced GaAs solar cells, Appl. Phys. Lett. **92**, 123512 (2008).

[43] Christopher G. Bailey, David V. Forbes, Ryne P. Raffaelle, and Seth M. Hubbard, Near 1 V open circuit voltage InAs/GaAs quantum dot solar cells, Appl. Phys. Lett. **98**, 163105 (2011).

[44] Christopher G. Bailey, David V. Forbes, Stephen J. Polly, Zachary S. Bittner, Yushuai Dai, Chelsea Mackos, Ryne P. Raffaelle, and Seth M. Hubbard, Open-circuit voltage improvement of InAs/GaAs quantum-dot solar cells using reduced InAs coverage, IEEE J. Photovolt. **2**, 269 (2012).

[45] A. Varghese, M. Yakimov, V. Tokranov, V. Mitin, K. Sablon, A. Sergeev, and S. Oktyabrsky, Complete voltage recovery in quantum dot solar cells due to suppression of electron capture, Nanoscale **8**, 7248 (2016).

[46] Kimberly A. Sablon, John W. Little, Vladimir Mitin, Andrei Sergeev, Nizami Vagidov, and Kitt Reinhardt, Strong enhancement of solar cell efficiency due to quantum dots with built-in charge, Nano Lett. **11**, 2311 (2011).